

## High Dynamic Range Spectral (HDRS) Image Database

The *ISET* package includes images from our high dynamic range spectral (HDRS) image database. These images are complete spectral approximations the light radiance field. The full HDRS image database includes a collection of additional images and customized software tools. This document describes the methodology we used to acquire the data and estimate the spectral radiance for the images in the HDRS database.

To create spectral radiance (photons/sec/nm/m<sup>2</sup>) HDRS images, the user combines linear sensor measurements from a calibrated camera with linear models of surfaces and illuminants. These data and models are combined to form an estimate of the multispectral image data.

The scene data were acquired with a 12-bit CCD 6 Megapixel camera. The process begins by acquiring eighteen different images, including six exposure durations and three color filter conditions. The data from these images are combined to estimate the scene radiance. The multiple filters expand the spectral dimension of the scene data; the multiple exposures expand the dynamic range of the scene data.

The high quality database of spectral images serves as a source of input data to the [virtual camera simulator](#). High dynamic range spectral data are essential in order to simulate accurately the effects of optics and sensors. Using a very high quality initial data set makes it possible to assess the properties of many other sensors whose dynamic range are limited compared to the HDRS database images.

### ***Linear representation of spectral radiance images***

The spectral radiance of a surface measures the rate of photons emitted (or scattered) from a surface as a function of area, angular direction, and wavelength. In most cases, such as for a simple reflective surface, a vector,  $s$ , represents the photons/sec/nm/m<sup>2</sup>, describes the spectral radiance. If we have measurements from 400 to 700nm, in 5 nm steps, then the vector  $s$  will have 61 entries. Representing such an images requires a lot of memory for images of any significant spatial size. For example, a 512 x 512 image with 16-bits per wavelength plane is stored in about 30 MB. A 1Kx1K image is stored in about 120 MB of data.

The spectral radiance functions in most natural images are regular functions of wavelength [1]. This makes it possible to use low-dimensional linear models to summarize efficiently the scene spectral radiance data. Specifically, the spectral representation of the light reflected from each point a scene can be approximated by a linear combination of a small set of spectral basis functions,  $B_i$ , where  $w_i$  are the weights

chosen to minimize the error between the spectral radiance and its linear model approximation, and  $N$  is the dimensionality of the spectral representation.<sup>1</sup>

$$s \approx \sum_{i=1}^N w_i B_i$$

If the number of basis functions,  $N$ , is much less than 61 then the low-dimensional linear models of spectral radiance are reduce the amount of data that must be stored. The accuracy of the low-dimensional spectral representations are limited by 1) how well the spectral radiance data conform to a low dimensional linear model, 2) the dimensionality of the image capture system which may or may not have enough sensors to capture the scene information, and 3) the quality of the algorithms for inferring the spectral radiance functions from the sensor data.

Data gathered over the last fifteen years suggests that for any given scene, containing only one or two light sources, the dimensionality of the spectral radiance functions will be accurately captured by five or six basis functions [2, 3, 4, 5, 6]. Hence, we captured image data from using a three-color camera in combination with three filters. One of the captures was made with no color filter, and two were made with different color filters placed between the camera and the scene. This procedure yields nine different spectral samples. The three different RGB images generate nine color channel values for each image pixel, enough for a reasonable approximation to many scenes.

In addition, we have learned that the dynamic range of the vast majority of natural scenes is on the order of 5000:1 if one excludes specular highlights [7]. Hence, a capture system based on a 12-bit ADC that uses multiple exposure durations to bracket the range can capture almost all of the information in most natural scenes [8, 9, 10].

We provide more detailed information about the methodology and algorithms for estimating the scene spectral radiance from the camera data in the following section.

---

<sup>1</sup>The complete characterization of the spectral radiance factor of a surface that has both diffuse and fluorescent components requires the full  $N \times N$  matrix,  $S$ , where  $N$  is the number of wavelength samples represented in the matrix  $S$ . If the surface is diffuse and does not fluorescence,  $S$  has values between 0 and 1 along the diagonal and no values in the off-diagonal positions in the matrix. Hence, a vector,  $s$ , corresponding to the diagonal component of  $S$ , can represent the spectral radiance of a diffuse surface.

## ***Multicapture methods***

### **Dynamic Range**

We used [a Nikon D100 digital SLR](#) camera with two carefully chosen filters to record high dynamic range multispectral<sup>2</sup> measurements of natural scenes. Because of its low noise and dark current, the Nikon D100 is close to a true 12-bit camera [7]. We used the Nikon D100's auto-bracketing function to take six images in rapid sequence at exposure settings separated by 2 stops. Used in this way, the Nikon D100's effective dynamic range is roughly 1,000,000:1.

For each scene, we captured six auto-bracketing pictures each with and without the two color filters in the imaging path. This resulted in a total of 18 images (6 exposure settings x 3 color filter conditions) for each scene. To avoid significant image registration problems, the aperture setting (F-stop) was fixed for all 18 images. The shortest exposure duration was set based on photometric measurements of the maximum luminance. The camera was positioned on a tripod for stability across the capture. The images were spatially registered when necessary, though very little camera motion was present. Stable scenes, without significant image motion, were selected.

The Nikon sensor contains a Bayer mosaic with two green, one red and one blue photodetector type. These measurements span comprise a 1012 x1517 grid. The images distributed in the ISET package are sub-sampled to a spatial resolution of 253x380. In the full database, various sampling rates can be selected under software control.

To estimate the intensity recorded by each pixel, we used the last sample before saturation (LSBS) algorithm [9]. This sample has the highest signal-to-noise ratio. From this estimate, we created a single high dynamic range image with 9 color channels.

### **Multispectral Imaging**

We used the 9-color high dynamic range images captured for each scene to estimate a spectral radiance image for that scene. Spectral power distributions of many natural images can be modeled as a linear combination of a relatively small (~5) set of spectral basis functions.

To improve the estimation of the spectral radiance of the image, we acquired a measurement of the spectral power distribution of the scene illumination. Using this measurement, we could simulate the light scattered from a standard test chart (the Macbeth Color Checker) and derive three scene basis functions for that illumination. We added two spectral basis functions to these, a DC and a linear ramp function (see Figures 1, 2 and 3, below). These functions are not orthogonal, but they are independent. Through empirical measurements, described below, we found that these basis functions provided a high quality representation of the image data.

Each HDRS image, then, includes a set of spectral basis,  $B_i$ , along with the basis coefficients or weights,  $w_i$ . The basis coefficients,  $w_i$ , are calculated from the nine color channels recorded by the multicapture imaging system.

We estimate the basis coefficients in the following way. We represent the wavelength information at 31 samples, from 400 to 700 nm in 10 nm steps. Let  $r$  be a 9x1 vector representing the output of nine color channels for a single pixel a sampled scene. Let  $T$  be a 9 x 31 matrix representing the spectral responsivities of the nine color channels in the image capture device. Let  $B$  be a 31 x 5 matrix representing scene spectral basis functions. Finally, let  $w$  be a 5x1 vector representing the weights on  $B$ . Then,

$$r = TBw$$

Solve for  $w$  using the pseudoinverse of  $TB$ ,

$$w = [TB]^{-1} r$$

**Validation**

Figures 1, 2 and 3 are examples of 5 spectral basis functions we used in linear model approximations for the spectral radiance measured from the 24 color patches in the Macbeth ColorChecker illuminated by daylight (Figure 1), tungsten (Figure 2) and fluorescent (Figure 3). In each case, we set the first two spectral basis functions to be a DC and ramp signal. The remaining 3 spectral basis functions correspond to the 3 most significant eigenvectors derived from the singular value decomposition (SVD) of the spectral radiance measured from the 24 surfaces illuminated by tungsten, daylight or fluorescent.

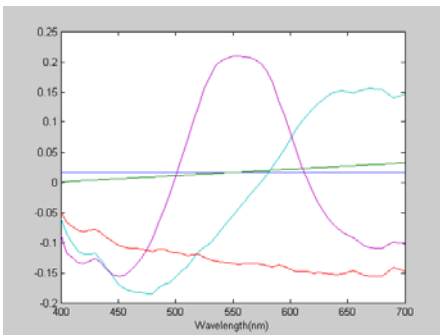


Figure 1: Spectral basis for surfaces illuminated by daylight

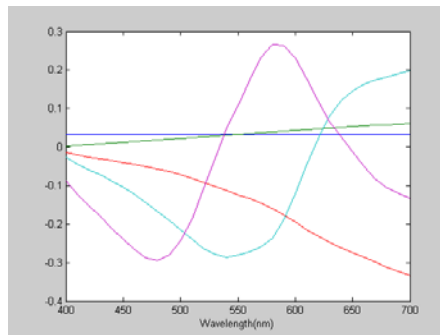


Figure 2: Spectral basis for surfaces illuminated by tungsten

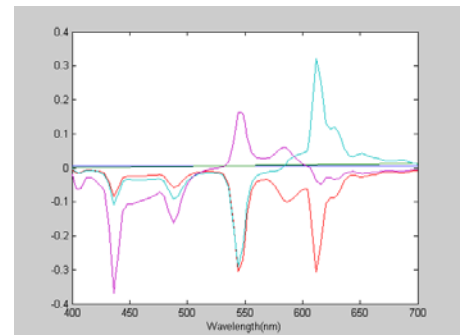


Figure 3: Spectral basis for surfaces illuminated by fluorescent

Figures 4, 5 and 6 compare the estimated (blue) and measured (red) spectral radiance of 24 color patches in the Macbeth Color Checker illuminated by daylight (Figure 4),

tungsten (Figure 5) and fluorescent (Figure 6). The RMSE between the estimated and measured data is less than 3.5 %, though in some parts of the spectrum, particularly above 650 nm, the Nikon D100 has poor wavelength sensitivity and the errors are significantly larger.

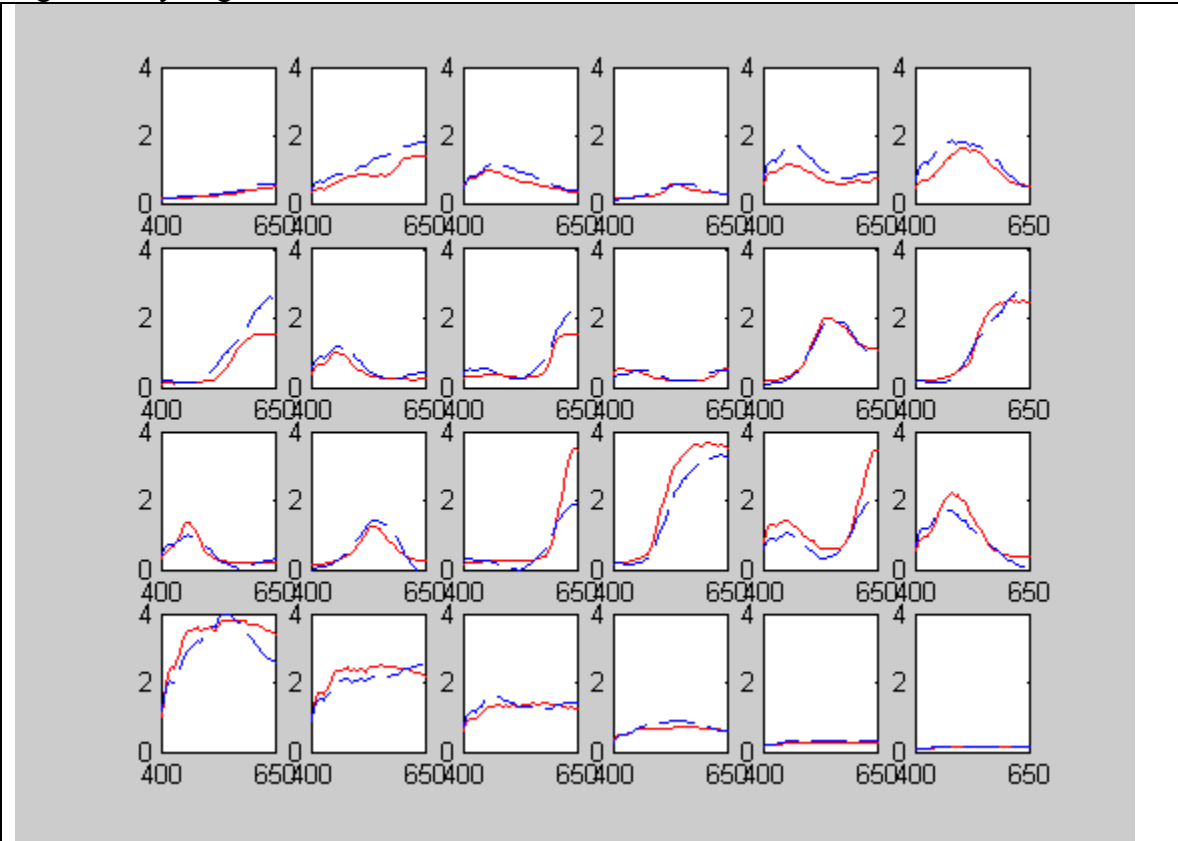


Figure 4: Spectral power distributions (red) and estimated spectral power distributions (blue) of the light scattered from the twenty-four surfaces of a Macbeth ColorChecker illuminated by daylight. The estimation was made using the five linear model basis functions shown in Figure 1 and data from the Nikon D100, as described in the text.

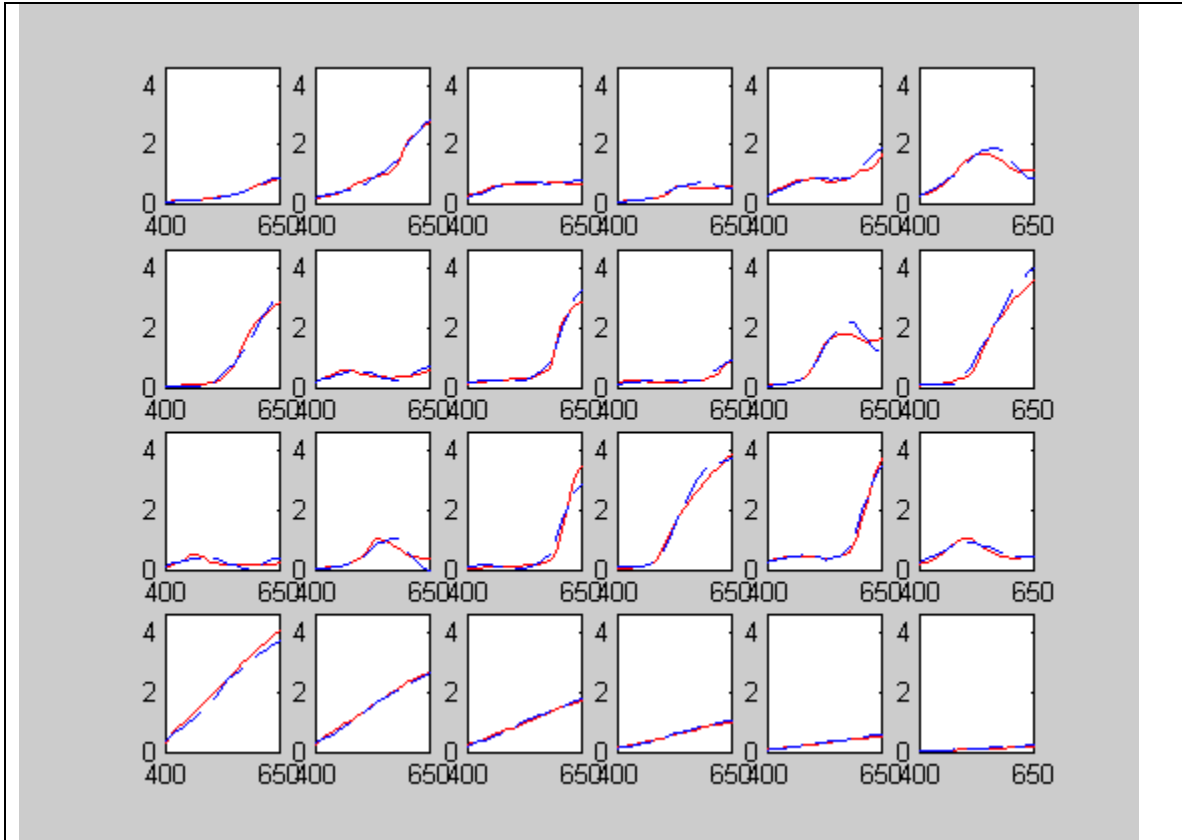


Figure 5: Spectral power distributions (red) and estimated spectral power distributions (blue) of the light scattered from the twenty-four surfaces of a Macbeth ColorChecker illuminated by a tungsten light. The estimation was made using the five linear model basis functions shown in Figure 2 and data from the Nikon D100, as described in the text.

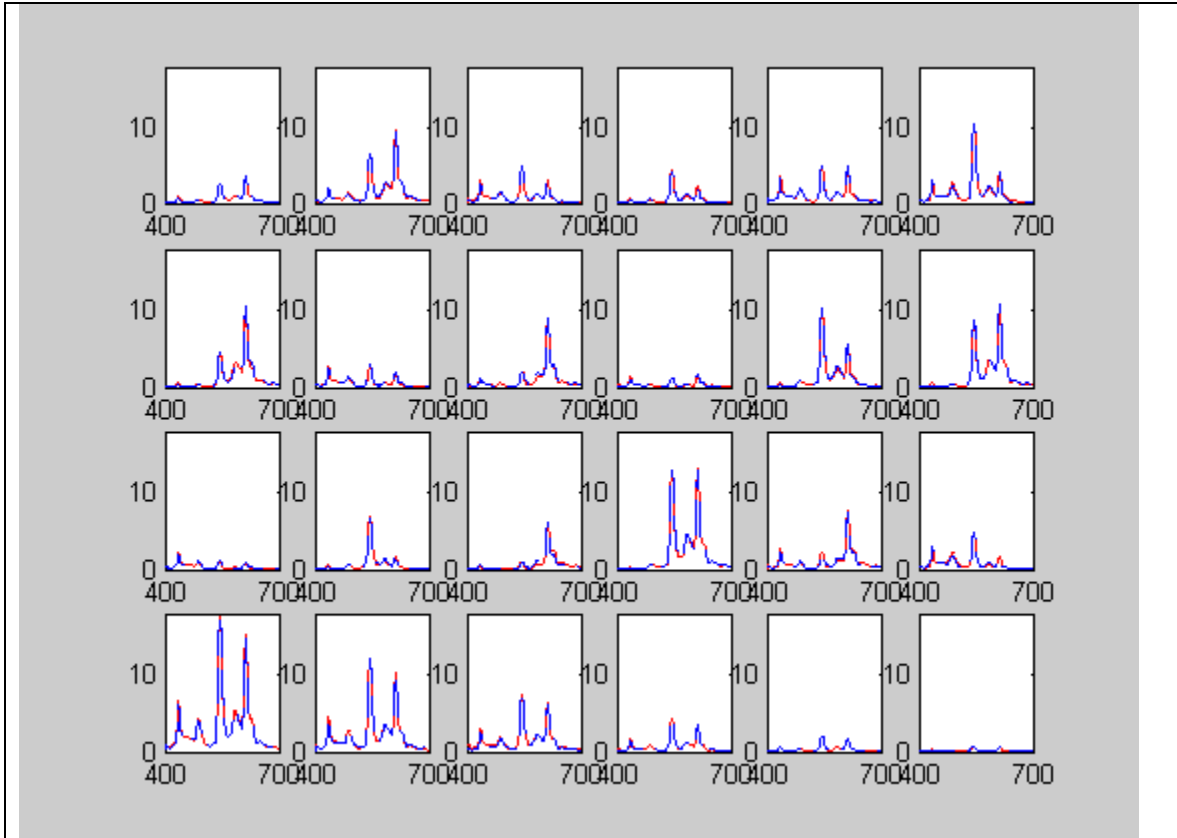


Figure 6: Spectral power distributions (red) and estimated spectral power distributions (blue) of the light scattered from the twenty-four surfaces of a Macbeth ColorChecker illuminated by a fluorescent light. The estimation was made using the five linear model basis functions shown in Figure 3 and data from the Nikon D100, as described in the text.

## References

[1] Wandell, B. A. (1995) *Foundations of Vision*, Sinauer Associates, Inc., p. 301

[2] D. B. Judd, D. L. MacAdam, and G. Wyszeski (1964) Spectral distribution of typical daylight as a function of correlated color temperature, *Journal of the Optical Society of America*, 54, pp.1031-1040.

[3] J. Cohen (1964) Dependency of the spectral reflectance curves of the Munsell color chips, *Psychonomic Society*, 1, pp. 369-370.

[4] Maloney, L. T. (1986) Evaluation of linear models of surface spectral reflectance with small number of parameters. *Journal of the Optical Society of America A*, 3, pp.1673-1683.

[5] D.H. Marimont and B.A. Wandell (1992) Linear models of surface and illuminant spectra, *Journal of the Optical Society of America A*, vol. 9, No. 11, pp. 1905.

- [6] C. C. Chiao, T.W. Cronin and D. Osorio (2000) Color signals in natural scenes: Characteristics of reflectance spectra and effects of natural illuminants, *Journal of the Optical Society of America A*, Vol 17, No. 2, pp. 218-224.
- [7] F. Xiao (2003) A system study of high dynamic range imaging (in preparation), Ph.D thesis, Stanford University.
- [8] P. E. Debevec and J. Malik (1997) Recovering High Dynamic Range Radiance Maps from Photographs, *Proc. SIGGRAPH'97*, pp. 369-378.
- [9] D. Yang, B. Fowler, A. El Gamal, and H. Tian (1999) A 640x512 CMOS Image Sensor with Ultrawide Dynamic Range Floating-Point Pixel-Level ADC, *IEEE Journal of Solid State Circuits*, vol. 34, pp.1821-1834.
- [10] B.A. Wandell., P. Catrysse, D. Yang and A. El Gamal [1999] Multiple Capture Single Image with a CMOS Sensor, *Chiba Conference on Multispectral Imaging*, pp. 11-17.